

Adsorption and corrosion inhibitive properties of P(2-aminobenzothiazole) on mild steel in hydrochloric acid media

S. S. Abd El Rehim¹ · S. M. Sayyah² · M. M. El-Deeb^{2,3} · S. M. Kamal^{2,4} · R. E. Azooz^{2,4}

Received: 31 March 2015 / Accepted: 17 November 2015 / Published online: 5 January 2016
© The Author(s) 2015. This article is published with open access at Springerlink.com

Abstract Corrosion inhibition of mild steel in hydrochloric acid solutions using electropolymerized Poly 2-aminobenzothiazole, P(2ABT), was evaluated using weight loss, potentiodynamic polarization and electrochemical impedance spectroscopy measurements at different temperature. Results showed that the inhibition efficiency increases with increasing the concentration of P(2ABT) up to $12.7 \times 10^{-6} \text{ mol L}^{-1}$ and decreases with raising the temperature. Polarization curves indicate that the studied compound acts as anodic inhibitor. Thermodynamic activation parameters for both dissolution and adsorption processes are calculated and discussed as well as the adsorption isotherms are calculated. Gibbs free energy value confirms the physical nature of the adsorption, also the mechanism of inhibition is discussed. Scanning electron microscopy is used to study the surface morphology of mild steel in hydrochloric acid solution in the absence and presence of $12.7 \times 10^{-6} \text{ mol L}^{-1}$ P(2ABT). Data obtained from all techniques are in a good agreement with each other.

Keywords Polymer · Corrosion inhibition · EIS · Mild steel · Adsorption isotherms

Introduction

The corrosion of metals, including mild steel, is a serious problem in many industries, especially during processes such as the pickling of steel, acid washing and etching [1, 2]. Corrosion inhibitors are chemical compounds that in small quantities can use in these processes to control the metal dissolutions. Most popular inhibitors are organic compound containing N, S, and O atoms. Organic compounds containing functional electronegative groups and π electrons in triple or conjugated double bonds are usually good inhibitors. The study of corrosion process and their inhibition by organic compounds is a very active field of research [3–5].

Benzothiazole and its derivatives are considered as one of the suitable compounds that be used as inhibitors due to it has donor atoms (N and S) via which bonding with metal ions can occur to form heterocyclic ring-metal complexes. These compounds are used as antioxidant, rust inhibitors and metal de-activators [6–9]. Aminothiazole derivatives have several useful properties like anti-corrosive [10], antimicrobial [11], antitumor activities [12] and used in sensing applications [13, 14].

Recently polymers have attracted considerable attention as corrosion inhibitors, and their inhibiting power is related structurally to the cyclic rings and hetero-atom (O, N and S) that are the major active centers of adsorption. A blanketing and protecting of the metal surface from corrosive agents present in the solution occurs via their functional groups which form complexes with metal ions [15].

✉ R. E. Azooz
re_azooz@yahoo.com

S. M. Sayyah
smsayyah@hotmail.com

¹ Chemistry Department, Faculty of Science, Ain Shams University, Cairo, Egypt

² Polymer Research Laboratory, Chemistry Department, Faculty of Science, Beni-Suef University, Beni Suef 62514, Egypt

³ Chemistry Department, Faculty of Science, Hail University, Hail 81451, Saudi Arabia

⁴ Chemistry Department, Collage of Science, Jazan University, Jazan 2097, Saudi Arabia

2-Aminothiazole has been polymerized both electrochemically [16–18] and chemically [19]. Homopolymers [20] and copolymers [21] of 2-aminobenzothiazole had been prepared by electropolymerization method. 2ABT [21] and other thiazole derivatives [22, 23] are used as a corrosion inhibitor for mild steel (MS) in HCl using different techniques, results show the inhibiting effect is due to adsorption of thiazols on MS surface.

The goal of this work is to investigate the electropolymerized P(2ABT) as a corrosion inhibitor for the acidic dissolution of mild steel in hydrochloric solution using weight loss, potentiodynamic polarization and electrochemical impedance spectroscopy measurements at different temperatures as well as thermodynamic activation parameters for both dissolution and adsorption processes will be calculated and discussed.

Experimental

Chemicals

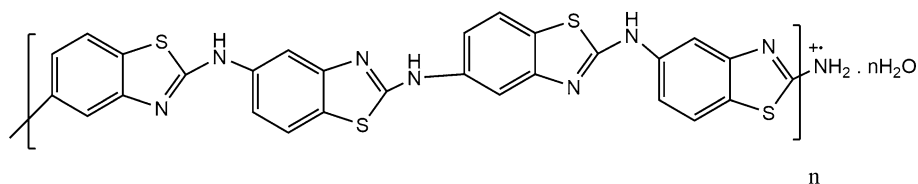
2-Aminobenzothiazole, HCl, Na₂SO₄, DMF are of grade reagent obtained from (Merck-Darmstadt, Germany). Poly 2-aminobenzothiazole P(2ABT) is prepared according to our previous work [20] and its structure is represented in Scheme 1.

Methodology

Weight loss measurements

Rectangular specimens of mild steel (MS), (wt%: 0.33 % C, 0.24 % Si, 0.52 % Mn, 0.04 %, Cr 0.02 % S and 98.5 % Fe) with size 3 cm × 4 cm × 0.2 cm were used as working electrode. Before each experiment, working electrodes are polished mechanically with SiC belts, 200–600 grit (Buehler, Ltd.), and 1 μm α-alumina (Buehler, Ltd.), washed with distilled water, then with acetone and dried. The weight loss, expressed in mg cm⁻², was determined by weighing the cleaned MS samples before and after immersion in HCl solution for 1 h in the absence and presence of various concentrations (2.1 × 10⁻⁶: 12.7 × 10⁻⁶ mol/L) (H₂O/DMF 98:2, v/v) of P(2ABT).

Scheme 1 Proposed structure of electropolymerized P(2ABT)



Potentiodynamic polarization measurements

Potentiodynamic polarization measurements are recorded using potentiostat/galvanostat Wenking PGS 95 connected with PC computer and performed in standard three electrode cell filled with 100 ml test solution with mild steel (2 cm⁻²) as working electrode, platinum wire as an auxiliary electrode and saturated calomel electrode as a reference electrode. Before each experiment, working electrode is polished with different emery paper in the normal way starting from coarse to fine, cleaned with distilled water, then with acetone and finally dried and *I*–*E* curves are recorded by computer software (Model ECT). For each experiment, a freshly prepared solution as well as a cleaned set of electrodes is used at constant temperature ±1° C using a circular water thermostat.

Electrochemical impedance spectroscopy measurements

Electrochemical impedance spectroscopy measurements are carried out on the open circuit potential (*E*_{ocp}), using a computer-controlled potentiostat (Voltalab). A frequency range of 100 kHz–100 MHz is used to obtain the impedance spectra after 1 h of immersion in the test solutions. A sine wave with 10 mV amplitude was used to perturb the system. The impedance diagrams are given in the Nyquist representation.

Surface morphology

The surface morphology of mild steel after 1 h of immersion in 1 M HCl solution in the absence and presence of 12.7 × 10⁻⁶ mol L⁻¹ P(2ABT) at constant temperature ±1° C is investigated using scanning electron microscopy model JXA-840A Electron Probe Microanalyzer (JEOL, Tokyo, Japan).

Results and discussion

Preparation and characterization

Electrooxidation of 1 × 10⁻³ M 2ABT in 0.05 M Na₂SO₄ and 0.3 M HCl at 309 K yield a good adhere P(2ABT) on the Pt-electrode, the obtained voltammogram is represented on Fig. 1 with two oxidation peaks (I and II) that

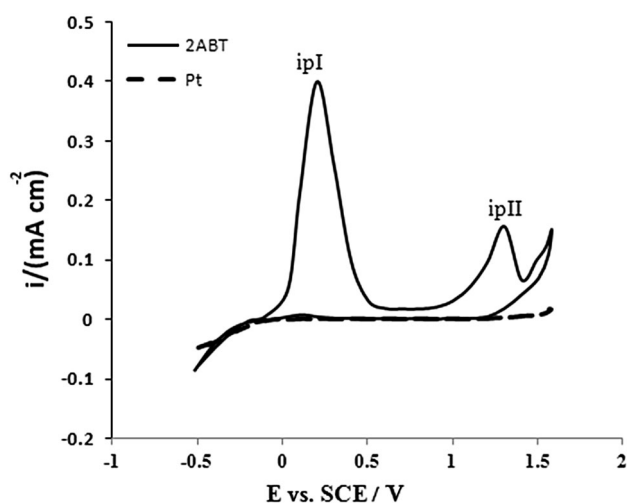


Fig. 1 Cyclic voltammogram of Pt-electrode from solution containing 0.3 M HCl and 0.05 M Na₂SO₄ at 309 K with scan rate of 25 mVs⁻¹ in absence and presence of 1 × 10⁻³ M 2ABT

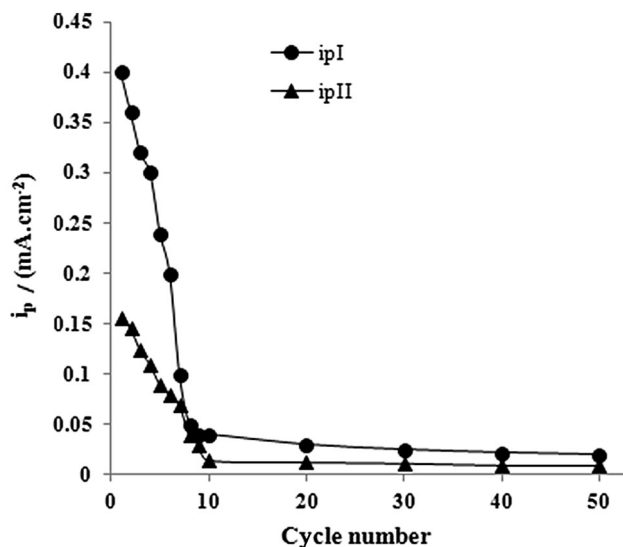


Fig. 2 Effect of number of cycles on the value of anodic current peaks I and II

developed in +200 and +1322 mV vs. (SCE) and no reduction peaks.

By increasing the number of cycles, the anodic current of both peaks decrease up to 50 cycles reflect the enhances of the deposited film stability and, therefore, the peak currents (I and II) decrease with repetitive cycling [21] as shown in Fig. 2.

By changing the scan rate both i_{pI} and i_{pII} increase as in Fig. 3 with linear regression equations:

$$i_{pI}(\text{mA}) = 0.149v^{0.5}(\text{mV s}^{-1})^{0.5} - 0.2499, r^2 = 0.991$$

$$i_{pII}(\text{mA}) = 0.010v^{0.5}(\text{mV s}^{-1})^{0.5} - 0.2476, r^2 = 0.988$$

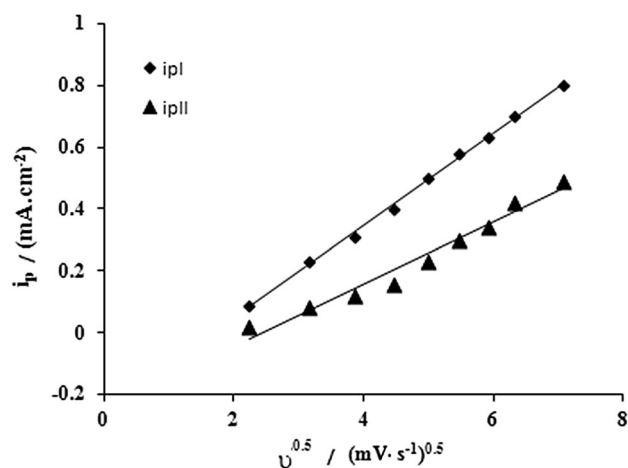


Fig. 3 Effect of (scan rate)^{0.5} on the value of anodic current peaks I and II

Both the two intercepts are small and negative which could be attributed to a decrease of the active area during the positive scan and the whole process is a partial diffusion process.

UV–vis spectra of the prepared polymer sample were measured using Shimadzu UV spectrophotometer (M160 PC) at room temperature in the range 200–900 nm using dimethyl-formamide as a solvent and reference. Spectra show the following:

- π – π^* transition at λ_{max} from 208 to 220 nm;
- polaron– π^* transition at $\lambda_{\text{max}} = 315$ nm and;
- π –polaron transition at $\lambda_{\text{max}} = 463$ nm.

IR measurements were carried out using Shimadzu FTIR-340 Jasco spectrophotometer (Japan) and show the following main bands:

- $\nu_{\text{max}} = 3402$ cm⁻¹ for NH₂ stretching vibration or OH strong hydrogen bonded group of H₂O molecules of hydration in P(2ABT);
- $\nu_{\text{max}} = 3064$ cm⁻¹ for CH stretching vibration of aromatic amine;
- $\nu_{\text{max}} = 1550$ cm⁻¹ for C=N stretching vibration;
- $\nu_{\text{max}} = 760$ cm⁻¹ for C=N stretching vibration in quinonoid form;
- $\nu_{\text{max}} = 618$ cm⁻¹ for C–S symmetric stretching vibration;
- $\nu_{\text{max}} = 721$ and 760 cm⁻¹ for C–S asymmetric stretching vibration.

From these methods, formation of P(2ABT) is confirmed [21].

The obtained P(2ABT) films were scratched from the Pt-electrode surface, washed with 0.3 M HCl to remove low molecular weight species and finally with double distilled water and left to dry at 90 C for 3 h then stored under vacuum until further studies.



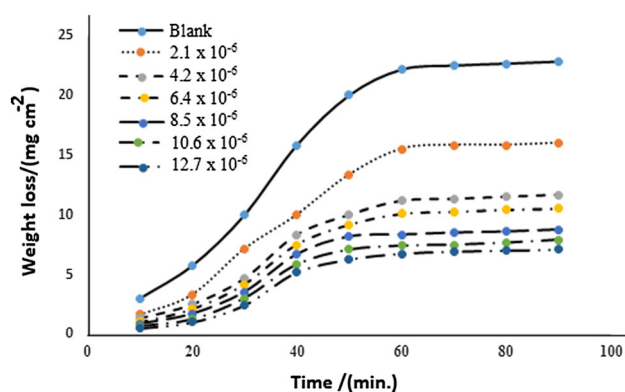


Fig. 4 Weight loss-time curves for MS in 1 M HCl in the absence and presence of different concentrations of P(2ABT) at 303 K

The solubility of the collected P(2ABT) was studied to find the suitable solvent to dissolve it, P(2ABT) did not dissolve completely in water, partially soluble in chloroform and acetone, but dissolve completely in DMF, DMSO and THF.

To prepare our inhibitor, a weighted amount of P(2ABT) was dissolved in 2 ml DMF and complete volume with water to form a mix solution [DMF: H₂O mix (2:98 v/v)]. The formed stock solution has a known concentration from which all used concentrations are taken via dilution.

Weight loss measurements

Effect of time

The variation of weight loss per area (mg cm^{-2}) of MS immersed in different time intervals up to 90 min in 1 M HCl solution at 303 K in the absence and presence of P(2ABT) is shown in Fig. 4. From the Figure, we notice that, the corrosion rate of MS coupons in free inhibitor solution increases with increasing the time up to 60 min, then begin to be mostly stable. By increasing the inhibitor concentrations, weight loss of MS in case of inhibitor solutions is lower than that of free inhibitor solution in the same

period of time. This behavior may be explained by the ability of the investigated compound to be used as an inhibitor through adsorption on MS surface and forming a barrier against the corrosive medium.

Effect of HCl concentration

The variety of weight loss (mg) and the corrosion rate, CR, ($\text{mg cm}^{-2} \text{h}^{-1}$) of MS immersed for 1 h in 0.5, 1.0 and 2.0 M HCl aerated stagnant solutions with and without various concentrations (from 2.1×10^{-6} to 12.7×10^{-6} M) of P(2ABT) at 303 K are calculated. The inhibition efficiency (%IE) values are calculated using Eq. (1) for MS in HCl acid solutions containing various concentrations of the P(2ABT). The calculated values of %IE are given in Table 1 and graphically represented in Fig. 5.

$$\text{IE}\% = \left(1 - \frac{W}{W^{\circ}}\right) \times 100 \quad (1)$$

where W° and W are the weight losses (g) for MS in the absence and presence of inhibitor.

From these data, the weight loss and the corrosion rate of MS electrode enhance with increasing the acid concentrations. On the other hand, addition of different concentrations of P(2ABT) inhibits the corrosion rate of MS in these solutions. This is clearly seen from the decrease in weight loss corresponding to a noticeable decrease in the corrosion rate in each acid concentration with an increase in the polymer concentrations. This trend may result from the fact that adsorption and surface coverage, θ , increases with the increase in P(2ABT) concentration; thus the MS surface is separated from the corrosive medium.

The use of P(2ABT) gives %IE ≈ 65 to 71 % for concentration 15 ppm ($12.7 \times 10^{-6} \text{ mol L}^{-1}$), which is better than that of the monomer (2ABT) which gives %IE ≈ 67 % for concentration of 50 ppm [22].

Figure 5 shows the variation of the calculated inhibition efficiency (%IE), values as a function of logarithmic concentration of the inhibitor. It is obvious from the data of Fig. 5

Table 1 Weight loss, corrosion rate of MS and inhibition efficiency %IE of various concentrations of P(2ABT) in 0.5, 1.0 and 2.0 M HCl at 303 K

P(2ABT) conc. $\times 10^{-6}$ (M)	Weight loss (mg)			Corrosion rate ($\text{mg cm}^{-2} \text{h}^{-1}$)			%IE		
	0.5 M	1.0 M	2.0 M	0.5 M	1.0 M	2.0 M	0.5 M	1.0 M	2.0 M
Blank	229.62	266.34	296.40	20.32	23.57	26.23	–	–	–
2.1	154.69	186.58	216.63	13.81	16.66	19.34	32.03	29.32	26.26
4.2	110.70	134.55	157.70	9.888	12.014	14.08	51.36	49.03	46.32
6.4	101.98	121.11	143.54	9.10	10.814	12.81	55.19	54.12	51.14
8.5	81.72	100.23	129.32	7.30	8.95	11.55	64.09	62.03	55.98
10.6	72.034	89.62	111.60	6.43	8.00	9.96	68.35	66.05	62.01
12.7	65.70	81.52	102.47	5.874	7.28	9.15	71.13	69.12	65.12

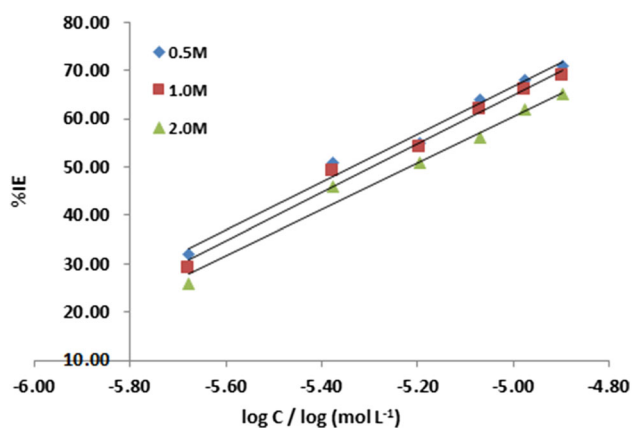


Fig. 5 The relation between %IE and log the concentration of P(2ABT) in different HCl concentrations at 303 K from weight loss technique

that, the inhibition efficiency increases with increasing the concentrations of the inhibitor. Moreover, it is found that at a given inhibitor concentration, the inhibition efficiency decreases in general with increasing the acid concentration.

Effect of temperature

The influence of solution temperature (298, 303 and 308 K) on the weight loss and consequently the corrosion rate, CR, of the MS electrode in 1.0 M HCl solution in the absence and presence of different concentrations of P(2ABT) were investigated. The immersion time of each experiment is 1 h. The values of weight loss (mg) and corrosion rate ($\text{mg cm}^{-2} \text{h}^{-1}$) are given in Table 2.

It is clear from the data that in the absence of the P(2ABT), the weight loss and consequently the corrosion rate of MS increase by raising the temperature, and decrease with increasing P(2ABT) concentrations.

The inhibition efficiencies (%IE) are calculated using Eq. (1) and are listed in Table 2.

Figure 6 represents the dependence of the inhibition efficiency (%IE) versus logarithmic the P(2ABT) concentrations in the three tested temperatures. According to

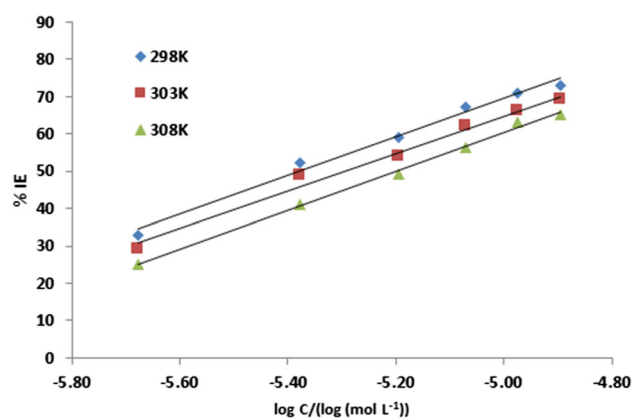


Fig. 6 The relation between %IE and log the concentration of P(2ABT) in 1.0 M HCl at 298, 303 and 308 K from weight loss technique

these data, it is seen that the inhibition efficiencies decrease with increasing the solution temperature. Such behavior could be due to the increases in the corrosion rate of MS and/or increasing the rate of desorption of P(2ABT) from the surface of MS with increasing temperature indicating that the inhibitor species are mainly physically adsorbed on the MS electrode surface.

Potentiodynamic polarization measurements

The potentiodynamic polarization behavior of MS electrode in 1.0 M HCl in the absence and presence of different concentrations of P(2ABT) with a scan rate of 10 mVs^{-1} at 298, 303 and 308 K is illustrated in Fig. 7.

As can be seen from the figure, the anodic and cathodic overpotentials are increased (mainly the anodic) in the presence of P(2ABT), meaning that the addition of P(2ABT) to HCl solution mainly reduces the anodic dissolution of MS and slightly retards the cathodic hydrogen evolution reaction. Based on this result, P(2ABT) is considerable, mainly acting as anodic inhibitor. The values of the corrosion current density, i_{corr} , and corrosion potential,

Table 2 Weight loss, corrosion rate of MS in 1.0 M HCl containing various concentrations of P(2ABT) and inhibition efficiency %IE at 298, 303 and 308 K

P(2ABT) conc. $\times 10^{-6}$ (M)	Weight loss (mg)			Corrosion rate ($\text{mg cm}^{-2} \text{h}^{-1}$)			%IE		
	298 K	303 K	308 K	298 K	303 K	308 K	298 K	303 K	308 K
Blank	240.92	266.34	283.86	21.32	23.57	25.12	–	–	–
2.1	159.96	186.58	210.98	14.28	16.66	18.84	33.01	29.32	25.01
4.2	159.96	186.58	210.98	10.21	12.01	14.79	52.12	49.03	41.12
6.4	114.34	134.55	165.65	8.73	10.81	12.73	59.03	54.12	49.32
8.5	97.83	121.11	142.58	7.01	8.96	11.01	67.12	62.03	56.18
10.6	78.51	100.23	123.28	6.18	8.00	9.27	71.02	66.05	63.08
12.7	69.20	89.62	103.87	5.73	7.28	8.76	73.12	69.12	65.13



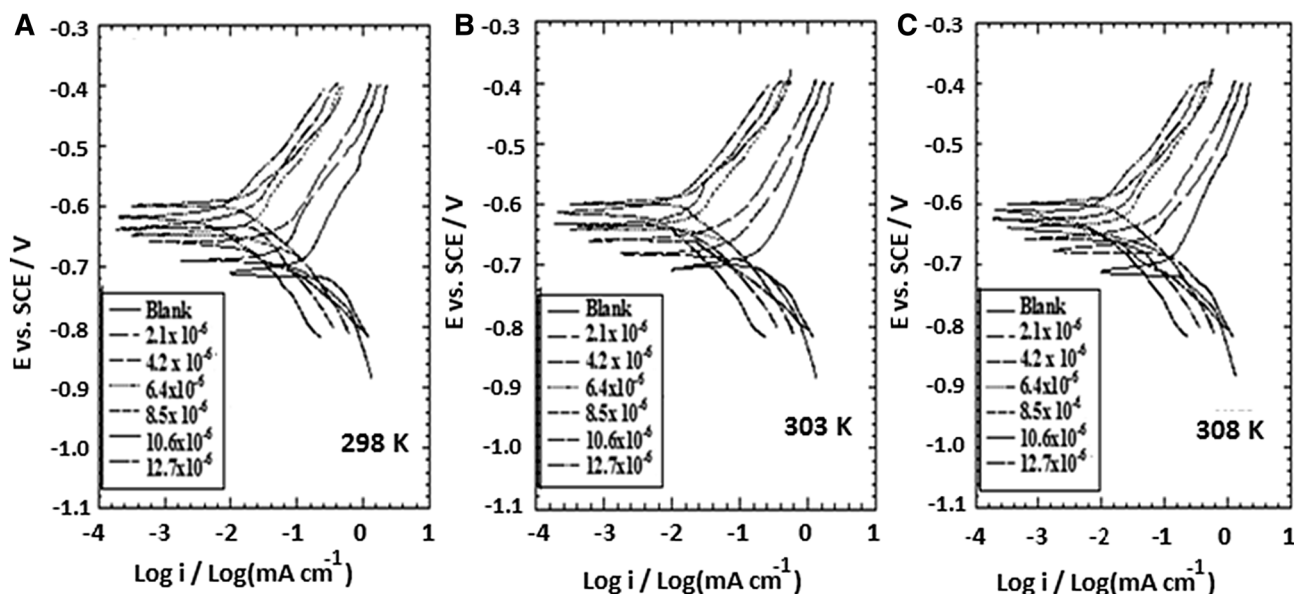


Fig. 7 Effect of P(2ABT) concentration on the potentiodynamic polarization curves of MS electrode in 1.0 M HCl at **a** 298 K, **b** 303 K and **c** 308 K

Table 3 The electrochemical kinetic parameters (i_{corr} , E_{corr} , β_c and β_a) and inhibition efficiency (%IE) obtained from polarization curves of MS electrode in 1.0 M HCl at 298, 303 and 308 K

P(2ABT) conc. $\times 10^{-6}$ (M)	i_{corr} (mA cm $^{-2}$)			$-E_{\text{corr}}$ (mV)			β_c (mV dec $^{-1}$)			β_a (mV dec $^{-1}$)			%IE		
	298 K	303 K	308 K	298 K	303 K	308 K	298 K	303 K	308 K	298 K	303 K	308 K	298 K	303 K	308 K
Blank	400	473.20	500	692	708	680	1.36	1.43	1.48	0.300	0.306	0.309	–	–	–
2.1	276	340.00	386	690	681	676	0.96	0.99	1.06	0.302	0.302	0.302	31.00	28.15	22.80
4.2	216	288.00	320	664	659	657	0.86	0.90	0.82	0.280	0.280	0.280	46.00	39.14	36.00
6.4	170	236.50	273	642	640	638	0.76	0.81	0.71	0.274	0.270	0.270	57.50	50.02	45.40
8.5	146	200.00	245	638	633	627	0.62	0.65	0.61	0.256	0.250	0.250	63.50	57.73	51.00
10.6	94	170.02	215.5	618	613	636	0.60	0.64	0.59	0.235	0.230	0.230	67.50	64.07	56.90
12.7	116.4	153.32	193.0	615	619	621	0.96	0.98	0.56	0.232	0.240	0.240	70.90	67.60	61.40

E_{corr} , for MS electrode in 1.0 M HCl solution in the absence and presence of P(2ABT) are determined by extrapolation of the cathodic and anodic Tafel lines to the point of intersection.

Table 3 represents the influence of P(2ABT) concentrations and temperatures on the corrosion parameters of MS electrode in 1.0 M HCl solution in the potential range ± 50 mV from the corrosion potential.

The inhibition efficiency (%IE) at different P(2ABT) concentrations and temperatures for MS electrode in 1.0 M HCl solution is calculated using Eq. (2). The values of %IE are given in Table 3.

$$\% \text{ IE} = \left(1 - \frac{i_{\text{corr}}}{i_{\text{corr}}^0} \right) \times 100 \quad (2)$$

According to these data, it is observed that at a given temperature, %IE increases with increasing the inhibitor concentration and decreases by raising the temperature. This behavior can be illustrated due to the desorption of some P(2ABT) species at higher temperatures. This suggests that physical adsorption may be the type of adsorption of the inhibitor on the metal surface. It is clear that the %IE values obtained from weight loss and polarization measurements are parallel in a good agreement.

Electrochemical impedance spectroscopy measurements

The impedance of the MS electrode in 1 M HCl solution at 298 K in the absence and presence of different

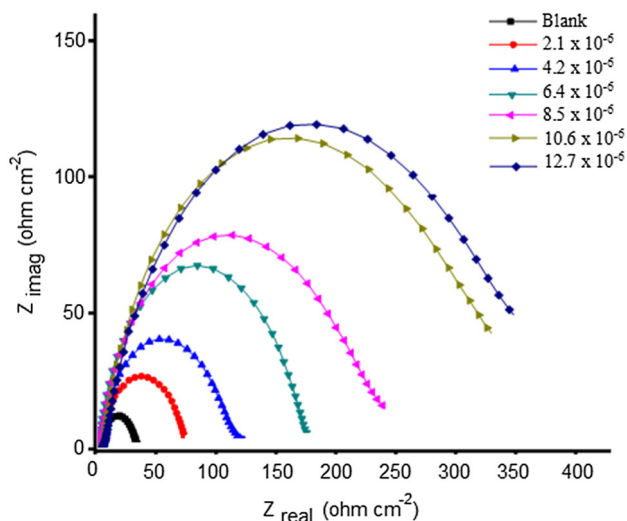


Fig. 8 Nyquist plots for MS in 1 M HCl at different concentrations of P(2ABT) at 298 K

concentrations P(2ABT) is shown in Fig. 8 as a Nyquist plot. Data show that, the presence of single semi-circle curves in all cases is attributed to the presence of single charge transfer process during dissolution of MS which is unaffected by the presence of inhibitor molecules. Deviations from perfect circular shape are referred to the frequency dispersion of interfacial impedance that arises due to surface roughness, impurities, dislocations, grain boundaries, adsorption of inhibitors, and formation of porous layers and in homogenates of the electrode surface [24]. EIS data show that, the R_{ct} values increase and the C_{dl} values decrease with increasing the inhibitor concentrations. This is due to adsorption of the inhibitor molecules on the MS and gradual replacement of water molecules, decreasing the extent of dissolution reaction of MS. The higher (R_{ct}) values are associated with slower corroding system [25]. The decrease in the C_{dl} can result from the decrease of the local dielectric constant and/or from the increase of the thickness of the electrical double layer suggested that the inhibitor molecules function by adsorption at the metal/solution interface [26]. The %IE obtained from EIS measurements is close to those deduced from polarization measurements.

Thermodynamic activation functions of the corrosion process

It has been reported elsewhere that, for the acid corrosion of MS, the logarithm of the corrosion rate given in $\text{mg cm}^{-2} \text{h}^{-1}$ (from weight loss data) and i_{corr} (from polarization data) is a linear function with $1/T$ where T is the absolute temperature [following Arrhenius Eq. (3) and the transition state Eq. (4)] [27].

$$\log(\text{CR}) = -\frac{E_a^0}{2.303RT} + A \quad (3)$$

$$\text{CR} = \frac{RT}{Nh} e^{\left(\frac{\Delta S^\circ}{R}\right)} e^{\left(-\frac{\Delta H^\circ}{RT}\right)} \quad (4)$$

where E_a^0 is the apparent activation energy, ΔS° is the entropy of activation, ΔH° is the enthalpy of activation, h is Planck's constant and N is the Avogadro number. According to Eq. 3, E_a^0 could be obtained by plotting $\log(\text{CR})$ against $1/T$ as in Fig. 9. Moreover, from Eq. 4, a plot of $\log(\text{CR}/T)$ against $1/T$ should give a straight line with a slope of $(-\Delta H^\circ/2.33 R)$ and an intercept of $(\log R/Nh - \Delta S^\circ/2.303 R)$ as in Fig. 10. The calculated parameters are given in Table 4. Inspection of these data reveals that the apparent activation energy E_a in HCl solution in the absence of P(2ABT) is $12.53 \text{ kJ mol}^{-1}$. The addition of a P(2ABT) to the acid solution increases E_a^0 and the extent of the increase is proportional to the inhibitor concentration, indicating that the energy barrier for the corrosion reaction increases with P(2ABT) concentration. This means that the corrosion reaction will be further pushed to surface sites that are characterized by progressively higher values of E_a^0 as the concentration of the P(2ABT) in the acid solution becomes larger. The entropy of activation ΔS° in the absence and presence of P(2ABT) is large and negative. This implies that the activated complex in the rate determining step represents an association rather than a dissociation step, meaning that a decrease in disordering takes place on going from reactants to the activated complex. The positive signs of ΔH° reflect the endothermic nature of the steel dissolution process. The data infer that the values of E_a^0 of the corrosion of MS in 1.0 M HCl solution in the presence of P(2ABT) are higher than that in the uninhibited acid solution. The thermodynamic functions E_a^0 , ΔH° and ΔS° enhance with increasing the inhibitor concentration, implying that more energy barrier for the corrosion in the presence of inhibitor is attained. Large and negative values of ΔS° imply that the activated complex in the rate determining step represents an association rather than dissociation step, meaning that the decrease in disordering takes place on going from reactants to the activated complex.

Adsorption considerations

Adsorption depends mainly on different parameters as; the charge, nature and electronic characteristics of the metal surface, adsorption of solvent and other ionic species, temperature of corrosion reaction and on the electrochemical potential at solution interface [28, 29].

Adsorption isotherms are usually used to describe the adsorption process, the most frequently used isotherms include; Langmuir, Frumkin, Hill de Boer, Parsons, Temkin, Flory–Huggins, Dhar-Flory–Huggins, Bockris-



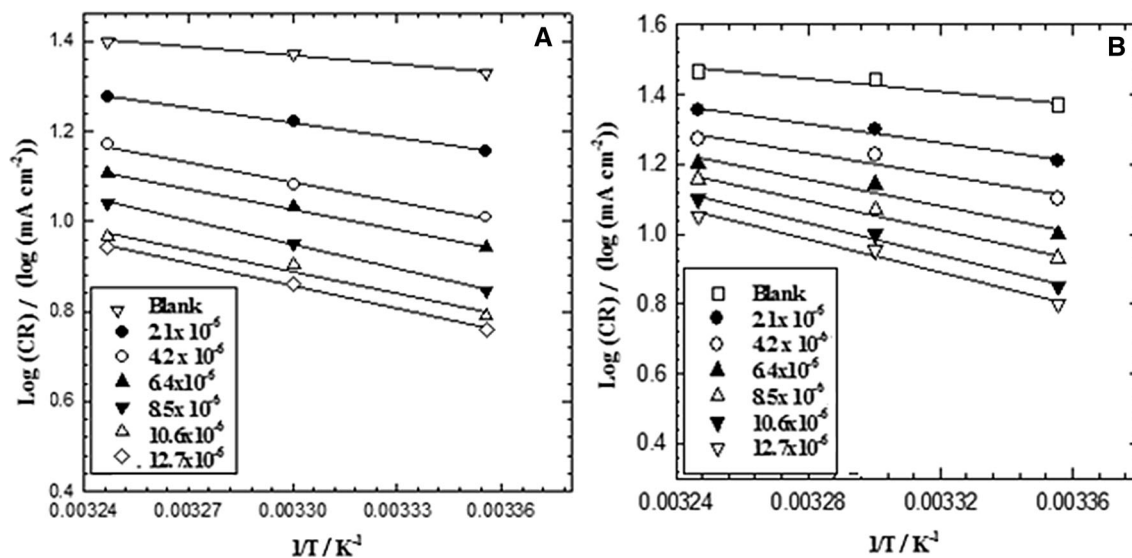


Fig. 9 Arrhenius plot of corrosion rate of MS in 1.0 M HCl containing various concentrations of P(2ABT) **a** from weight loss and **b** from polarization measurements

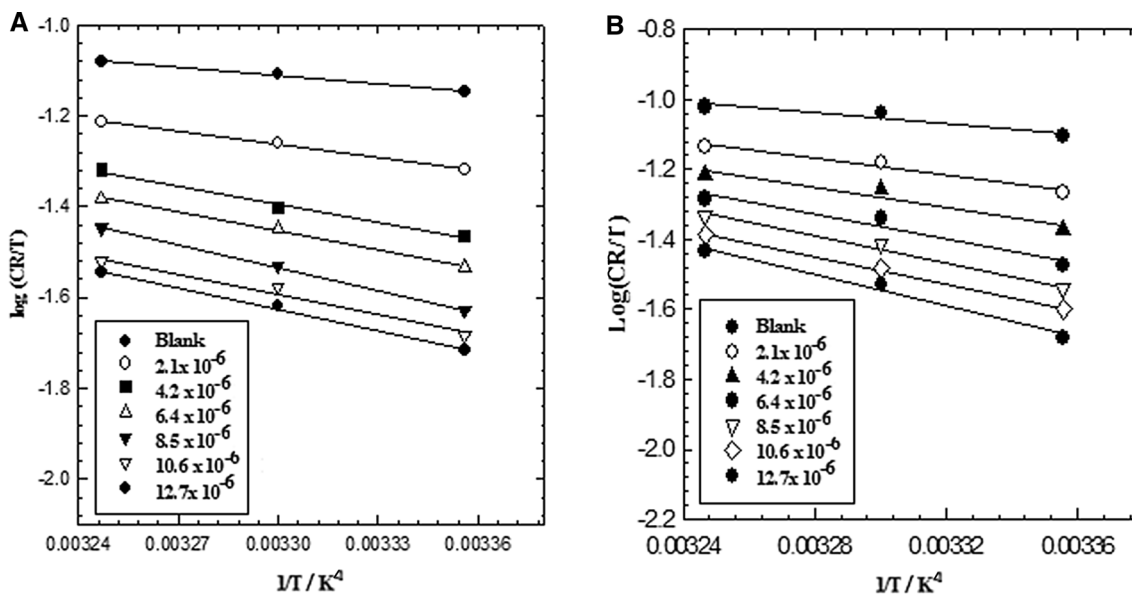


Fig. 10 Transition state plot of corrosion rate of MS in 1.0 M HCl containing various concentrations of P(2ABT) **a** from weight loss and **b** from polarization measurements

Swinkels and the recently formulated thermodynamic/kinetic model of El-Awady et al. [30–32] Adsorption isotherms can provide important information about the nature of the metal/inhibitor interaction. Adsorption of the organic molecules occurs as the interaction energy between inhibitor and metal surface is higher than that between the H_2O molecule and the metal surface [33].

To obtain the adsorption isotherm, the degree of surface coverage (θ) for various concentrations of the P(2ABT) is calculated according to ($\theta = \%IE/100$).

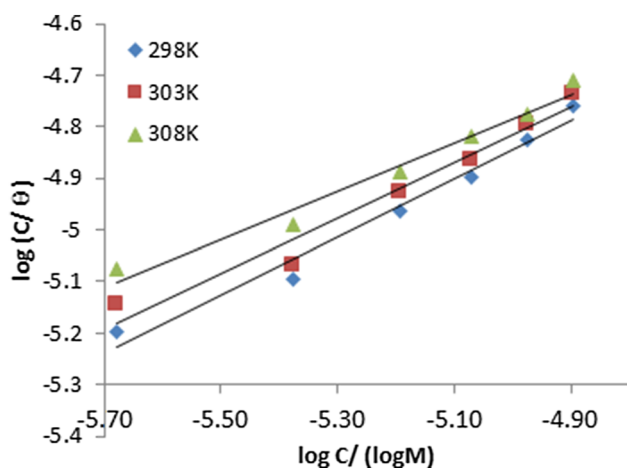
Because, the data of weight loss and polarization are close to each other, we use the data obtained from weight loss to study the adsorption of P(2ABT) on MS electrode in hydrochloric acid solution, different isotherms are studied as follows:

Langmuir adsorption isotherm is expressed according to Eq. (5) or its related one (6) [34, 35].

$$\frac{C}{\theta} = \frac{1}{K_{ads}} + C \quad (5)$$

Table 4 The thermodynamic activation functions of MS dissolution in 10 M HCl in the absence and presence of different concentrations of P(2ABT) obtained from weight loss and polarization data by applying Arrhenius and transition state plots

P(2ABT) conc. $\times 10^{-6}$ (M)	Weight loss			Polarization		
	E_a° (kJ mol $^{-1}$)	ΔH° (kJ mol $^{-1}$)	ΔS° (J mol $^{-1}$ K $^{-1}$)	E_a° (kJ mol $^{-1}$)	ΔH° (kJ mol $^{-1}$)	ΔS° (J mol $^{-1}$ K $^{-1}$)
Blank	12.53	11.24	-182.07	17.08	14.55	-187.81
2.1	21.08	18.61	-160.43	25.62	23.11	-144.16
4.2	28.28	25.71	-139.37	30.06	27.55	-131.14
6.4	28.76	26.23	-138.80	36.23	33.70	-112.56
8.5	30.62	27.92	-133.82	39.54	37.03	-102.80
10.6	31.04	28.53	-131.52	42.68	38.41	-100.42
12.7	32.40	29.87	-130.18	25.62	43.08	-84.99

**Fig. 11** Langmuir adsorption isotherm of P(2ABT) based on weight loss data at different temperatures

$$\log\left(\frac{C}{\theta}\right) = \log C - \log K_{\text{ads}} \quad (6)$$

where C is the concentration of the inhibitor, K_{ads} is the adsorption equilibrium constant and θ is degree of surface coverage of the inhibitor. Plotting $\log(C/\theta)$ against $\log C$ gives a linear relationship as shown in Fig. 11. The parameters of Langmuir isotherm are listed in Table 5. The r^2 values >0.96 indicate fitting to Langmuir adsorption isotherm [36], so the adsorption of P(2ABT) on the MS surface show no interaction between them [37].

For Temkin adsorption isotherm, the degree of surface coverage (θ) is related to inhibitor concentration (C) according to Eq. (7) and its log form (8) [34].

$$\exp(-2a\theta) = K_{\text{ads}}C \quad (7)$$

$$\theta = \frac{-2.303 \log K_{\text{ads}}}{2a} - \frac{2.303 \log C}{2a} \quad (8)$$

where K_{ads} is the adsorption equilibrium constant and a , is the attractive parameter. Temkin plots are presented in

Fig. 12, linear relationship, which shows that adsorption data fitted Temkin adsorption isotherm. Adsorption parameters obtained from Temkin adsorption isotherms are recorded in Table 5. The values of attractive parameter (a) are negative in all cases, indicating that repulsion exists in the adsorption layer.

Flory–Huggins adsorption isotherm can be expressed according to Eq. (9) [36], and is shown in Fig. 13.

$$\log\left(\frac{\theta}{C}\right) = \log K_{\text{ads}} + x \log(1 - \theta) \quad (9)$$

where the size parameter is x (the number of adsorbed water molecules substituted by a given inhibitor molecule). The value of the size parameter x is positive as shown in Table 5, indicating a bulky adsorption of P(2ABT) species which displace more than one water molecule from the MS surface.

Frumkin adsorption isotherm is given by Eq. (10) [34].

$$\log\left\{[C] \times \left(\frac{\theta}{1-\theta}\right)\right\} = 2.303 \log K_{\text{ads}} + 2\alpha\theta \quad (10)$$

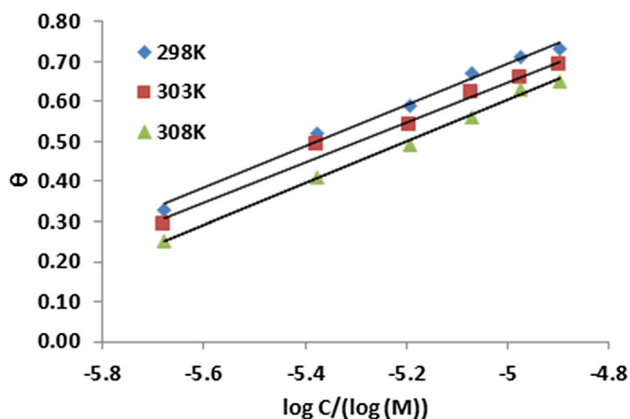
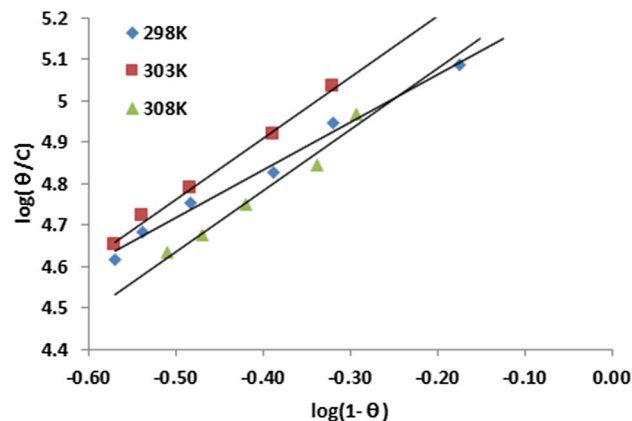
where K_{ads} is the adsorption–desorption constant and α is the lateral interaction term describing the interaction in adsorbed layer. A linear plot is seen (see Fig. 14) which show the applicability of Frumkin isotherm. The values for Frumkin adsorption parameters were recorded in Table 5. From which the value of the adsorption parameter α is positive, suggesting the attractive behavior of the inhibitor on the surface of mild steel. The characteristics of the El-Wady's kinetic/thermodynamic isotherm model are given by Eq. (11).

$$\log\left(\frac{\theta}{1-\theta}\right) = \log K + y \log C \quad (11)$$

where C is the concentration of the P(2ABT), θ is the degree of surface coverage, K_{ads} is the equilibrium constant of adsorption process and $K_{\text{ads}} = K^{1/y}$. The values for the

Table 5 Isotherms parameter from different models for adsorption of P(2ABT) based on weight loss data at different temperatures

Isotherm	Temperature (K)	r^2	Log K	ΔG_{ads} (kJ mol $^{-1}$)	a	α	x	$1/y$
Langmuir	298	0.97	-2.037	-21.58				
	303	0.96	-2.132	-22.49				
	308	0.97	-2.443	-24.69				
Frumkin	298	0.99	-0.000357189	-9.95		1.88		
	303	0.97	-0.00044949	-10.12		3.03		
	308	0.96	-0.000453775	-10.28		3.24		
Tempkin	298	0.99	1.28	-17.54	-0.45			
	303	0.99	1.19	-17.03	-0.44			
	308	0.99	1.26	-17.43	-0.45			
Flory-Huggin	298	0.99	5.30	-30.71			1.15	
	303	0.99	5.50	-31.91			1.47	
	308	0.98	5.37	-31.15			1.47	
EL-Awady	298	0.92	1.05	-15.95				1.05
	303	0.985	1.09	-16.45				1.09
	308	0.996	1.04	-16.41				1.04

**Fig. 12** Timkin adsorption isotherm of P(2ABT) based on weight loss data at different temperatures**Fig. 13** Flory-Huggins adsorption isotherm of P(2ABT) based on weight loss data at different temperatures

El-Awady's kinetic/thermodynamic model parameters were recorded in Table 5. This model is plotted in Fig. 15.

Gibb's free energy, enthalpy of adsorption and entropy of adsorption can be calculated from the adsorption isotherm [36–40]. Standard Gibb's free energy ($\Delta G_{\text{ads}}^{\circ}$) can be calculated using Eq. (12):

$$\Delta G_{\text{ads}}^{\circ} = -RT \ln(K_{\text{eq}}) \quad (12)$$

where K_{eq} is an equilibrium adsorption constant which is calculated from the adsorption isotherm to be followed and it has been calculated with reference to its molars of water, 55.5 M, under standard condition. Data are inserted into Table 5.

A negative $\Delta G_{\text{ads}}^{\circ}$ suggest that the adsorption of P(2ABT) onto the MS surface is a spontaneous process [41] and strongly attracted to MS [42]. Generally, values of

$\Delta G_{\text{ads}}^{\circ}$ up to -20 kJ mol $^{-1}$ are consistent with physisorption, while those around -40 kJ mol $^{-1}$ or higher are associated with chemisorptions [43]. So, we suggest from the data in Table 5 that the adsorption is physically in natures.

From standard free energy, enthalpy and entropy of adsorption can be calculated using the following Eq. (13) or its log form (14):

$$\Delta G_{\text{ads}}^{\circ} = \Delta H_{\text{ads}}^{\circ} - T\Delta S_{\text{ads}}^{\circ} \quad (13)$$

$$\log K_{\text{eq}} = \frac{-\Delta H_{\text{ads}}^{\circ}}{2.303RT} + \frac{\Delta S_{\text{ads}}^{\circ}}{2.303RT} - \log 55.5 \quad (14)$$

Values of $\Delta H_{\text{ads}}^{\circ}$ and $\Delta S_{\text{ads}}^{\circ}$ are obtained and illustrated in Table 6. The magnitude of the values of $\Delta H_{\text{ads}}^{\circ}$ and $\Delta S_{\text{ads}}^{\circ}$ is characteristic of the occurrence of the replacement process during adsorption process



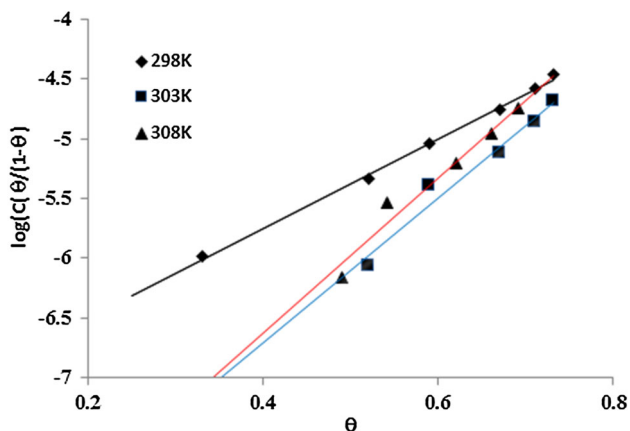


Fig. 14 Frumkin adsorption isotherm of P(2ABT) based on weight loss data at different temperatures

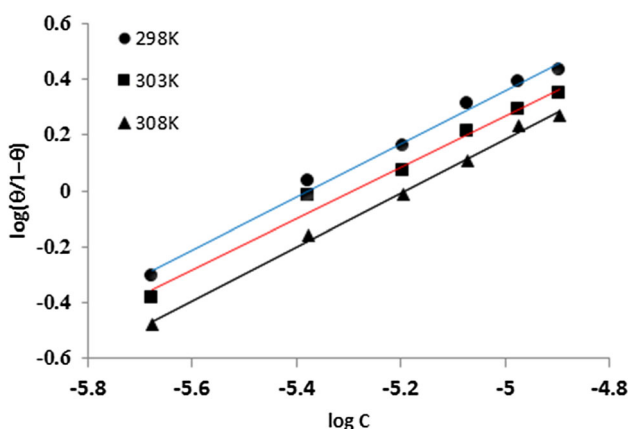


Fig. 15 El-Awady adsorption isotherm of P(2ABT) based on weight loss data at different temperatures

Surface morphology

SEM photographs of mild steel after 1 h of immersion in 1 M HCl solution in the absence and presence of $12.7 \times 10^{-6} \text{ mol L}^{-1}$ P(2ABT) at constant temperature $\pm 1^\circ \text{ C}$ are shown in Fig. 16a–c. Data show that, the Polished lines of the steel surface are observed before exposure to the corrosive medium (Fig. 16a) while the damage of its surface after immersion in 1 M HCl due to the dissolution is seen in Fig. 16b. SEM image (Fig. 16c) of mild steel surface after immersion in 1 M HCl in the presence of P(2ABT) shows the smooth surface indicating that the inhibitor molecules hinders the dissolution of MS by forming the protective film on its surface and thereby reduce the corrosion rate.

Mechanism of inhibition

Corrosion of iron and steel [44, 45] in HCl solution follows the following proposed mechanism

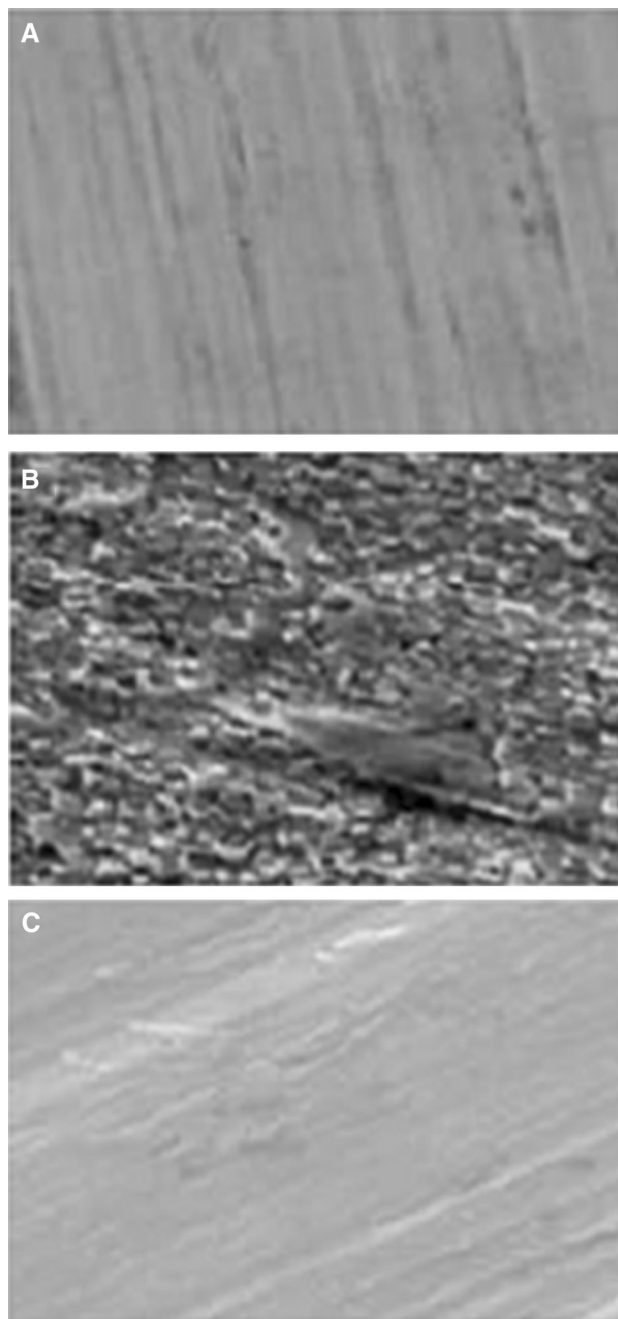
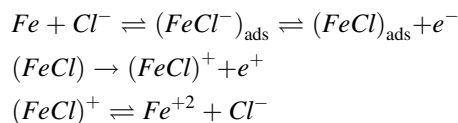


Fig. 16 SEM micrographs of mild steel samples at 28 K **a** only surface polishing, **b** after immersion in 1 M HCl without inhibitor, **c** after immersion in 1 M HCl in presence of $12.7 \times 10^{-6} \text{ M}$ P(2ABT)

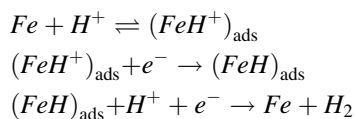
1. Anodic dissolution of iron is as follows:



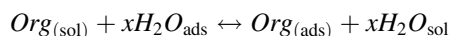
2. Cathodic hydrogen evolution is as follows:

Table 6 Values of $\Delta H_{\text{ads}}^{\circ}$ and $\Delta S_{\text{ads}}^{\circ}$ from different isotherm models of P(2ABT) based on weight loss data

Isotherm	$\Delta H_{\text{ads}}^{\circ}$ (kJ mol ⁻¹)	$\Delta S_{\text{ads}}^{\circ}$ (JK ⁻¹ mol ⁻¹)
Langmuir	71.13	38.29
Frumkin	3.68	73.01
Temkin	1.67	73.38
Flory-Huggin	-12.64	89.01
EL-Awady	1.67	73.38



Accumulated ions at the metal/solution interface replace solvent molecules from the metal surface and their centers reside at the inner Helmholtz plane. The anions are adsorbed when the metal surface has an excess positive charge in an amount greater than that required to balance the charge corresponding to the applied potential [46]. The exact nature of this interaction depends on the relative coordinating strength towards the given metal of the particular groups present [46]. Due to the well accepted model, the adsorption of organic inhibitor molecules is often a displacement reaction involving removal of adsorbed water molecules from the metal surface [43].



In general, the proceeding of physical adsorption requires the presence of both electrically charged metal surface and charged species in the bulk of the solution. Chemisorption process involves sharing or transfer of charge from the inhibitor molecules to the metal surface to form a coordinate type of a bond. This is a possible in case of a positive as well as a negative charge on the surface [47].

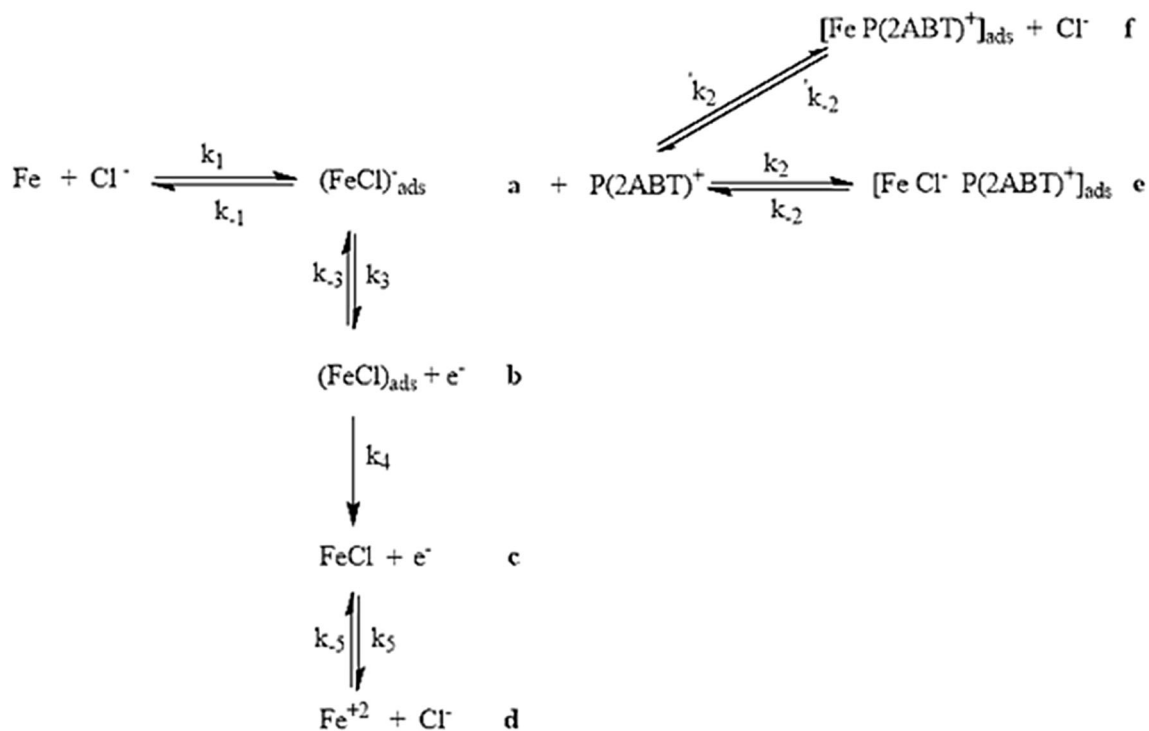
When mild steel immersed in the HCl solution, in the presence of P(2ABT), Cl⁻ ions are firstly adsorbed to the MS surface create an excess negative charge towards the solution (step a), and favor more adsorption of the cations [41, 44]. After that Two assumptions are proposed;

I.

P(2ABT)⁺ are adsorbed on (Fe-Cl)⁻ surface (step e). So it can be proposed that, reaction, pathway of P(2ABT) seems to be through (a → e). The equilibrium constant k_2 must be much bigger than k_3 ($k_2 \gg k_3$) and reaction (a → e) should be more favoured than (a → d). Thus, the P(2ABT) may act as a barrier against corrosion of MS (see Scheme 2).

II.

P(2ABT)⁺ replaces with Cl⁻. Thus, Cl⁻ ion is removed from the metal surface towards a solution (Scheme 2). As a result of this, a new double layer is formed so MS is

**Scheme 2** Proposed adsorption mechanism of P(2ABT) onto MS surface in HCl solution

loaded negative charge against positive charged P(2ABT) to form $(\text{Fe P}(2\text{ABT})^+)_{\text{ads}}$.

Depending on this explanation, the equilibrium constant of the related step k'_2 is expected higher than both k_2 and k_3 . Consequently, P(2ABT) interacts with the MS surface other than electrostatic interactions, it can be suggested that the reaction pathway is from step (a \rightarrow f) instead of (a \rightarrow e).

Conclusions

From the overall experimental results the following conclusions can be deduced:

1. P(2ABT) is a good inhibitor for MS corrosion and acts as anodic type inhibitor in HCl solutions.
2. Gravimetric and electrochemical measurements show that the inhibiting action increases with increasing the inhibitor concentration and decreases with raising the temperature.
3. Gibbs free energy value confirms the spontaneous physical adsorption.
4. The energy barrier for the corrosion reaction increases with the addition of P(2ABT).
5. The adsorption of P(2ABT) on the MS surface in HCl solutions follows the tested isotherms.

Open Access This article is distributed under the terms of the Creative Commons Attribution 4.0 International License (<http://creativecommons.org/licenses/by/4.0/>), which permits unrestricted use, distribution, and reproduction in any medium, provided you give appropriate credit to the original author(s) and the source, provide a link to the Creative Commons license, and indicate if changes were made.

References

1. Revie RW, Uhlig HH (2008) Corrosion and corrosion control an introduction to corrosion science and engineering. Wiley, New Jersey
2. Eddy NO, Ita BI (2011) QSAR, DFT and quantum chemical studies on the inhibition potentials of some carbozones for the corrosion of mild steel in HCl. *J Mol Model* 17(2):359–376
3. El-Deeb MM, Sayyah SM, Abd El-Rehim SS, Mohamed SM (2015) Corrosion inhibition of aluminum with a series of aniline monomeric surfactants and their analog polymers in 0.5 M HCl solution: Part II: 3-(12-sodiumsulfonate dodecyloxy) aniline and its analog polymer. *Arab J Chem* 8(4):527–537
4. John S, Joseph BA (2012) Electro analytical, surface morphological and theoretical studies on the corrosion inhibition behavior of different 1,2,4-triazole precursors on mild steel in 1 M hydrochloric acid. *Mater Chem Phys* 133(2–3):1083–1091
5. Sayyah SM, El-Deeb MM, Abd El-Rehim SS, Ghanem RA, Mohamed SM (2014) Experimental and theoretical evaluation on the effect of the terminal side chain of a polymeric surfactant on the inhibition efficiency of aluminum corrosion in acid medium. *Port Electrochim Acta* 32:417–429
6. Ajmal M, Mideen AS, Quraishi MA (1994) Quraishi, 2-hydrazino-6-methyl-benzothiazole as an effective inhibitor for the corrosion of mild steel in acidic solutions. *Corros Sci* 36(1):79–84
7. Samide A, Bibicu I, Rogalski MS, Preda M (2005) Study of the corrosion inhibition of carbon-steel in dilute ammoniacal media using N-ciclohexil-benzothiazole-sulphenamida. *Corros Sci* 47(5):1119–1127
8. Rajendran S, Sridevi SP, Anthony N, Amalraj AJ, Sundearavadivelu M (2005) Corrosion behaviour of carbon steel in polyvinyl alcohol. *Anti Corross Methods Mater* 52(2):102–107
9. Popova A, Christov M (2006) Evaluation of impedance measurements on mild steel corrosion in acid media in the presence of heterocyclic compounds. *Corros Sci* 48(10):3208–3221
10. Popova A (2007) Temperature effect on mild steel corrosion in acid media in presence of azoles. *Corros Sci* 49(5):2144–2158
11. Cruz J, Garcia-Ochao E, Castro M (2003) Experimental and theoretical study of the 3-amino-1,2,4-triazole and 2-aminothiazole corrosion inhibitors in carbon steel. *J Electrochem Soc* 150(1):B26–B35
12. Cukurovalı A, Yılmaz I, Ahmedzade M, Kirbag S (2001) Antimicrobial activity studies of the metal complexes derived from cyclobutane-substituted thiazole carbamate ligands. *Heteroat Chem* 12(7):665–670
13. Zhou X, Shao L, Jin Z, Liu J-B, Dai H, Fang J-X (2007) Synthesis and antitumor activity evaluation of some schiff bases derived from 2-aminothiazole derivatives. *Heteroat Chem* 18(1):55–59
14. Filho NLD, Do Carmo R, Rosa AH (2006) An electroanalytical application of 2-aminothiazole-modified silica gel after adsorption and separation of Hg (II) from heavy metals in aqueous solution. *Electrochim Acta* 52(3):965–972
15. Alcantara L, Roldan PS, Margionte AL, Castro GR, Padilha CCF, Flo-rentino AO, Padilha PM (2004) Determination of Cu, Ni and Pb in aqueous medium by FAAS after pre-concentration on 2-aminothiazole modified silica gel. *J Braz Chem Soc* 15(3):366–371
16. Solmaz R, Kardas G (2009) Electrochemical synthesis and characterization of poly-2-aminothiazole. *Prog Org Coat* 64(1):81–88
17. Venancio EC, Costa CAR, Machado SAS, Motheo AJ (2001) AFM study of the initial stages of polyaniline growth on ITO electrode. *Electrochem Commun* 3(5):229–233
18. Ciftci H, Testereci HN, Oktem Z (2011) Electrochemical polymerization of 2-aminothiazole. *Polym Bull* 66:747–760
19. Yıldırım M, Kaya I (2012) A comparative study of aminothiazole-based polymers synthesized by chemical oxidative polymerization. *Synth Met* 162(5–6):436–443
20. Sayyah SM, Azooz RE (in press) Electrosynthesis and characterization of adherent poly(2-aminobenzothiazole) on Pt-electrode from acidic solution. *Arab J Chem*. doi:10.1016/j.arabjc.2011.06.031
21. Sayyah SM, Abd El-Rehim SS, Kamal SM, El-Deeb MM, Azooz RE (2011) Electropolymerization kinetics of a binary mixture of *o*-phenylenediamine and 2-aminobenzothiazole and characterization of the obtained polymer films. *J Appl Polym Sci* 119(1):252–264
22. Patel NS, Beranek P, Nebyla M, Přibyl M, Šnita D (2014) Inhibitive effects by some benzothiazole derivatives on mild steel corrosion in 1 N HCl. *Int J Electrochem Sci* 9:3951–3960
23. Hur E, Varol GA, Gorguni K, Sakarya HC (2011) Inhibition of acidic corrosion of low carbon steel by novel synthesized benzothiazole derivatives. *GU J Sci* 24(4):699–707
24. Osman MM, Omar AM, Al-Sabagh AM (1997) Corrosion inhibition of benzyl triethanol ammonium chloride and its ethoxylate



- on steel in sulphuric acid solution. *Mater Chem Phys* 50(3):271–274
25. Raspini IA (1993) Influence of sodium salts of organic acids as additives on localized corrosion of aluminum and its alloys. *Corrosion* 49(10):821–828
 26. Schmitt G, Bedbur K (1985) Investigations on structural and electronic effects in acid inhibitors by AC impedance. *Werkst Korros* 36(6):273–280
 27. Khadom A, Yaro AS, Kadum AAH, AlTaie AS, Musa AY (2009) The effect of temperature and acid concentration on corrosion of low carbon steel in hydrochloric acid media. *Am J Appl Sci* 6(7):1403–1409
 28. Rozendeld L (1981) *Corrosion inhibitors*. Mc Graw-Hill, New York
 29. Obot IB, Obi-Egbedi NO, Umoren SA (2009) Ginseng root: a new efficient and effective eco-friendly corrosion inhibitor for aluminium alloy of type AA 1060 in hydrochloric acid solution. *Int J Electrochem Sci* 4:863–877
 30. Kamis E (1990) The effect of temperature on the acidic dissolution of steel in the presence of inhibitors. *Corrosion* 46(6):476–484
 31. Abd El-Rehim SS, Magdy A, Ibrahim M, Khaled F (1999) 4-Aminoantipyrine as an inhibitor of mild steel corrosion in HCl solution. *J Appl Electrochem* 29(5):593–599
 32. Abu Al-Ola KAA, Al-Nami SY (2011) 1-Benzoyl-4-phenyl-3-thiosemicarbazide as corrosion inhibitor for carbon steel in H₃PO₄ solution. *Mod Appl Sci* 5(3):193–206
 33. Moretti G, Quartarone G, Tassan A, Zingales A (1994) Inhibition of mild steel corrosion in 1N sulphuric acid through indole. *Werkst Korrosion* 45(12):641–647
 34. Bilgic S, Caliskan N (2001) An investigation of some Schiff bases as corrosion inhibitors. *J Appl Electrochem* 31(1):79–83
 35. Shockry H, Yuasa M, Sekine I, Issa RM, El-baradie HY, Gomma GK (1998) Corrosion inhibition of mild steel by Schiff base compounds in various aqueous solutions: part 1. *Corros Sci* 40(12):2173–2186
 36. Acharya S, Upadhyay SN (2004) The inhibition of corrosion of mild steel by some fluoroquinolones in sodium chloride solution. *Indian I Metals* 57(3):297–306
 37. Ashassi-Sorkhabi H, Majidi MR, Seyyedi K (2004) Investigation of inhibition effect of some amino acids against steel corrosion in HCl solution. *Appl Surf Sci* 225(1–4):176–185
 38. Aliji Novi LJ, Gotovac V (1985) Adsorption and corrosion inhibition properties of thymol. *J Appl Electrochem* 15(5):767–770
 39. Ashassi-Sorkhabi H, Shaabani B, Seifzadeh D (2005) Corrosion inhibition of mild steel by some schiff base compounds in hydrochloric acid. *Appl Surf Sci* 239(2):154–164
 40. Szyprowski AJ (2000) Relationship between chemical structure of imidazoline inhibitors and their effectiveness against hydrogen sulphide corrosion of steels. *Br Corros J* 35(2):155–160
 41. Tang L, Li X, Lin L, Mu G, Liu G (2006) The effect of 1-(2-pyridylazo)-2-naphthol on the corrosion of cold rolled steel in acid media: Part 2: Inhibitive action in 0.5 M sulfuric acid. *Mater Chem Phys* 97(2–3):301–307
 42. Mu G, Li X, Liu G (2005) Synergistic inhibition between tween 60 and NaCl on the corrosion of cold rolled steel in 0.5 M sulfuric acid. *Corros Sci* 47:1932–1952
 43. Moretti G, Guidi F, Grion G (2004) Tryptamine as a green iron corrosion inhibitor in 0.5 M deaerated sulphuric acid. *Corros Sci* 46(2):387–403
 44. Yurt A, Balaban A, Kandemir SU, Bereket G, Erk B (2004) Investigation on some Schiff bases as HCl corrosion inhibitors for carbon steel. *Mater Chem Phys* 85(2–3):420–426
 45. Yurt A, Duran B, Dal H (2014) An experimental and theoretical investigation on adsorption properties of some diphenolic Schiff bases as corrosion inhibitors at acidic solution/mild steel interface. *Arab J Chem* 7(5):732–740
 46. Gao B, Zhang X, Sheng Y (2008) Studies on preparing and corrosion inhibition behaviour of quaternized polyethyleneimine for low carbon steel in sulfuric acid. *Mater Chem Phys* 108(2–3):375–381
 47. Popova A, Sokolova E, Raicheva S, Christov M (2003) AC and DC study of the temperature effect on mild steel corrosion in acid media in the presence of benzimidazole derivatives. *Corros Sci* 45(1):33–58

